Experimental Gerontology 108 (2018) 77–86

Contents lists available at ScienceDirect

Experimental Gerontology

journal homepage: www.elsevier.com/locate/expgero

# Spermidine ameliorates the neuronal aging by improving the mitochondrial function in vitro

Yu-Hong Jing[a,b], Ji-Long Yan[c], Qing-Jun Wang[c], Hai-Chao Chen[c], Xue-Zhu Ma[a], Jie Yin[a], Li-Ping Gao[c,*]

[a] Institute of Anatomy and Histology & Embryology, Neuroscience, School of Basic Medical Sciences, Lanzhou University, No. 199 of Donggang West Road, Lanzhou City, Gansu province 730000, PR China

[b] Key Laboratory of Preclinical Study for New Drugs of Gansu Province, Lanzhou University, No. 199 of Donggang West Road, Lanzhou City, Gansu province 730000, PR China

[c] Institute of Biochemistry and Molecular Biology, School of Basic Medical Sciences, Lanzhou University, No. 199 of Donggang West Road, Lanzhou City, Gansu province 730000, PR China

ARTICLE INFO

Section editor: Christian Humpel

*Keywords:*
Mitochondria
Spermidine
Nerve cells
Aging

ABSTRACT

Changes in mitochondrial structure and function are the initial factors of cell aging. Spermidine has an antiaging effect, but its effect on neuronal aging and mitochondrial mechanisms is unclear. In this study, mouse neuroblastoma (N2a) cells were treated with D-galactose (D-Gal) to establish cell aging to investigate the antiaging effect and mechanisms of spermidine. Changes in the cell cycle and β-galactosidase activity were analyzed to evaluate the extent of cell aging. Stabilities of mitochondrial mRNA and mitochondrial membrane potential (MMP) were evaluated in the process of cell aging under different treatments. The mitochondrial function was also evaluated using the Seahorse Metabolic Analysis System combined with ATP production. The unfolded protein response (UPR) of the N2a cells was analyzed under different treatments. Results showed that spermidine pretreatment could delay the cell aging and could maintain the mitochondrial stability during D-Gal treatment. Spermidine increased the proportion of cells in the S phase and maintained the MMP. The oxygen utilization and ATP production in the N2a cells were reduced by D-Gal treatment but were partially rescued by the spermidine pretreatment. Spermidine ameliorated the N2a cell aging by promoting the autophagy and inhibiting the apoptosis except the UPR. These results showed that spermidine could ameliorate the N2a cell aging by maintaining the mitochondrial mRNA transcription, MMP and oxygen utilization during the D-Gal treatment.

## 1. Introduction

Aging is the most important risk factor for neurodegenerative diseases. Neurodegenerative diseases, such as Parkinson disease (PD) and Alzheimer's disease (AD), exhibit typical age-dependent characteristics (de Lau et al., 2004; Rubinsztein and Easton, 1999). This point suggests that the factors accelerating aging are also involved in the development of neurodegenerative diseases. The mechanisms of aging are complex and many factors were involved, such as genomic stability decline, epigenetic change, nutritional disorders, proteolysis abnormality, telomere shortening, stem cell depletion and mitochondrial dysfunction (Gems and Partridge, 2013; Kenyon, 2010; Lopez-Otin et al., 2013). Among of them, mitochondrial function decline is a critical factor in neuronal aging, which is attributed to the high oxygen consumption in the process of neuron metabolism (Lopez-Otin et al., 2016; Macedo et al., 2017). Recently, mitochondrial dysfunction was found to be involved in the development of brain aging (Basha and Poojary, 2014), especially mitochondrial DNA (mtDNA) mutation and fragment deletion, which existed in the early times (Lauri et al., 2014). In one study, mice with abnormal mtDNA repair exhibited a typical aging phenotype in the postnatal period for two months and shortening of whole life span (Trifunovic et al., 2004). The protective effect of free radical scavengers on the mitochondria is also the main mechanism of antiaging and in reducing neurodegenerative diseases (Sano et al., 1997; Zhao et al., 2008).

Spermidine is a trivalent cationic compound containing amino groups in eukaryotic cells. It is synthesized by butanediamine and *S*-adenosylmethionine (Gosule and Schellman, 1976). Under normal

*Abbreviations:* PD, Parkinson disease; AD, Alzheimer's disease; mtDNA, mitochondrial DNA; D-Gal, D-galactose; Rh123, Rhodamine 123; OCR, oxygen consumption rate; N2a, mouse neuroblastoma cell; MTT, 3-4,5-dimethyl-2-thiazolyl-2,5-diphenyl-2-H-tetrazolium bromide; MMP, mitochondrial membrane potential

* Corresponding author.
*E-mail address:* Gaolp@lzu.edu.cn (L.-P. Gao).

https://doi.org/10.1016/j.exger.2018.04.005
Received 6 December 2017; Received in revised form 5 April 2018; Accepted 6 April 2018
Available online 09 April 2018
0531-5565/ 

conditions, spermidine is alkaline and exists as protonated forms under physiological conditions. Spermidine can interact with nucleic acids, proteins, ATP and other polyanions through electrostatic binding, and is involved in multiple functions, such as maintenance of DNA genomic homeostasis, gene transcription and translation regulation, regulation of cell proliferation, and maintenance of cell survival (Childs et al., 2003; Pegg, 1988). In the central nervous system, polyamines (spermidine and spermine) accumulate preferentially in glial cells but not in neurons (Biedermann et al., 1998; Laube and Veh, 1997). By contrast, Krauss et al. reported that polyamine synthesis is absent in glia cells but its heterogeneous expression predominantly localized to neurons and neuropil (Krauss et al., 2007). This phenomenon suggests that brain obtains polyamines from external sources; but inside the brain, the major sources of polyamines are the glial cells that store them (Skatchkov et al., 2000; Skatchkov et al., 2014). Spermidine exerts a protective effect on the neuronal oxidative stress, inflammation and local ischemia injury through the inhibition of histone acetyltransferase activity, reduction of histone-3 acetylation and regulation of specific gene expression (Minois et al., 2012). Spermidine regulates cell growth, differentiation and death and also stabilizes DNA and RNA structures and various biological membranes (Wang et al., 2009). Spermidine is an antioxidant, nutrient and the second messenger in cells (Khomutov et al., 2009). It can induce cell autophagy and prolong the life spans of yeast, fruit fly, nematode and human immune cells (Eisenberg et al., 2009; Soda et al., 2009). Recently, Bell et al. reported that the protective effect of pentylenetetrazole in a model of epilepsy depends on the increase of putrescine which is the simplest polyamine, then the putrescine converted into the GABA in the presynaptic neurons. This results demonstrated polyamine has unknown roles in the development brain. (Bell et al., 2011). In another study, Noro et al. reported that spermidine promoted retinal ganglion cell survival and optic nerve regeneration by inhibiting the active microglia and inflammation (Noro et al., 2015). These evidences suggested Potential roles of polyamine are complex in nervous system and need to be investigated.

Spermidine can ameliorate the damage from oxidative stress in aging mice and upregulate the autophagy activity through chromatin acetylation to anti-aging in yeast, fruit fly, nematodes, and human cells (Minois, 2014). Target elimination of abnormal mitochondria depends on autophagy activity. Nevertheless, little is known whether spermidine can maintain the mitochondrial stability under stress conditions through mitochondrial quality control, thereby delaying the neuronal aging. The aim of the present study is to determine the effect of spermidine on neuronal aging and its protective mechanisms.

## 2. Materials and methods

### 2.1. Reagent

D-Galactose (D-Gal, catalog no. G0625), D-glucose (catalog no. 552003), D-mannitol (catalo no. 240184), spermidine (catalog no. 85561), 3-4,5-dimethyl-2-thiazolyl-2,5-diphenyl-2H-tetrazolium bromide (MTT, catalog no. M5655) and Rhodamine 123 (Rh123, catalog no. R8004) were purchased from Sigma (St. Louis, MO, USA); The β-galactosidase staining kit and protein extraction kit were purchased from Beyotime (Beyotime Biotechnology Co., Ltd., Shanghai, China; catalog no. c0602); The ATP assay kit was purchased from Jiancheng Biotechnology (Jiancheng Biological Company, Nanjing, China; catalog no. A095-1). The oxygen consumption rate (OCR) assay kit was purchased from Agilent (Agilent Co., Ltd., IL, US; catalog no. 103020-100). The calf serum was purchased from Sijiqing Biotechnology (Sijiqing Biotechnology Company, Hangzhou, China). The polyclonal anti-rabbit P53 antibodies were purchased from Abcam (Abcam, Cambridge, UK; catalog no. ab131442). The polyclonal anti-rabbit cleaved caspase-3 (catalog no. Asp175), AMPK (catalog no. 2532) and phosphorylation AMPK antibodies (catalog no. 2531S) were purchased from cell signaling (CST, MA, USA). The polyclonal anti-rabbit LC3 antibody was purchased from Santa Cruz (Santa Cruz, IL, USA; catalog no. sc292354); The monoclonal anti-mouse GAPDH antibody was purchased from Millipore (Millipore, CA, USA; catalog no. AB2302). The RNAiso Plus kit (catalog no. 9108), PrimeScript RT Master Mix kit and SYBR Premix Ex Taq II kit (catalog no. RR036A) were purchased from TAKARA (TAKARA Biotechnology Co., ltd., Dalian, China). The primers were designed and synthesized by TAKARA (TAKARA Biotechnology Co., ltd., Dalian, China).

### 2.2. MTT test

The mouse neuroblastoma cell (N2a) line was purchased from the Shanghai Cell Institute of the Chinese Academy of Sciences. The complete medium was composed of DMEM high glucose medium and 10% calf serum; the pH value was 7.4; the cell growth in the logarithmic phase was cultured in a 96-well plate; and the cell density was adjusted to $1.5 \times 10^4$/well. After adherence, cells were incubated with at 5, 10, 20 and 30 μM spermidine. After 1 h, the original culture solution was sucked, and the cells were gently washed with the DMEM complete medium twice. Then, the cells were incubated with 50, 100, 200, and 300 mM D-Gal for 24 h and 48 h as described in previous work (Delwing-de Lima et al., 2017; Li et al., 2014; Xing et al., 2006; Zhang et al., 2015). In brief, D-Gal, D-glucose, and D-mannitol were diluted directly in DMEM and sterilized using a bacterial filter. The volume of solution was modified according to the final concentration. The cell viability was measured using the MTT assay. In brief, cells were incubated with 450 μM MTT for 3 h and then centrifuged at 1800 rpm for 10 min at room temperature to remove the supernatant. Afterwards, formazan was extracted from pelleted cells with 600 μl of DMSO for 15 min. The amount of MTT-formazan was determined by 570 nm absorbance with 655 nm as the wavelength reference. To evaluate the effects of 100 mM spermidine on osmosis of N2a cells, N2a cells were incubated with the 100 mM D-glucose and D-mannitol for 48 h and then the cell viability was measured using MTT assay.

### 2.3. β-Galactosidase staining

N2a cells were treated with 20 μM spermidine. After 1 h, spermidine was washed off, and the cells were incubated with the 100 mM D-Gal for 48 h. In the control groups, N2a cells were incubated with 100 mM D-Gal, 100 mM D-glucose, and 100 mM D-mannitol for 48 h, repectively, but without the spermidine-pretreatment. The original culture medium was removed, and the cells were gently rinsed twice at 37 °C with 0.01 M PBS (pH, 7.4). A total of 200 μl of fixed solution per well was added, and the mixture was incubated at room temperature for 15 min. The fixed solution was removed and rinsed with 0.01 M PBS for 5 min. Another 200 μl of β-galactosidase staining solution per well was added, and the mixtures was incubated overnight. After removing the staining solution and rinsing with 0.01 M PBS, the number of positive cells was counted in nine areas of view per well under an inverted microscope.

### 2.4. Cell cycle analysis

N2a cells were treated with 5, 10, 20 and 30 μM spermidine. After 1 h, spermidine was washed off, and 100 mM of D-Gal was added. The cells were incubated for 48 h, harvested, fixed with 70% ethanol, stained with propidium iodide and detected using flow cytometry. The percentages of cells in the S, G1, and G2 phase were calculated.

### 2.5. ATP determination

N2a cells were incubated with 5, 10, and 20 μM spermidine. After 1 h, the spermidine was washed off, and 100 mM of D-Gal was added. The cells were incubated for 48 h and then harvested for ATP determination. The operation was performed according to the kit instruction. The absorbance of each well was detected using a microplate

reader (exciting light of 636 nm). ATP concentration was calculated according to the following formula:

ATP (μmol/g protein) = (OD value of the treated group − OD value of the control group) × sample protein concentration (g prot/l) / (OD value of the standard sample − OD value of the blank well) × standard sample concentration ($1 \times 10^3$ μmol/l) × dilution ratio.

### 2.6. Mitochondrial membrane potential (MMP) analysis

N2a cells were incubated with 5, 10, and 20 μM spermidine. After 1 h, spermidine was washed off, and 100 mM of D-Gal was added. The cells were incubated for 48 h and then were harvested for the MMP analysis. Rh123 storage solution was diluted to 1.5 μg/ml concentration with 0.01 M PBS (pH 7.4) as the work solution. The cells were rinsed with 1 ml of 0.01 M cooling PBS. A total of 500 μl of Rh123 working solution was added and developed for 30 min at 37 °C in the dark. Then, the cells were centrifuged at 800 rpm for 10 min and washed with 0.01 M ice cold PBS twice. The cells were suspended with 0.01 M PBS and measured using flow cytometry.

### 2.7. OCR assay

The OCR assay was performed using a Clark-type electrode (Agilent, Seahorse XF24 analyzer) in accordance with previous methods (Yao et al., 2009). In brief, the N2a cells were incubated with 20 μM spermidine. After 1 h, the spermidine was washed off, and 100 mM of D-Gal was added. The cells were cultured for 48 h. On the day of the metabolic flux analysis, The medium was changed to unbuffered DMEM (DMEM base medium supplemented with 25 mM glucose, 1 mM sodium pyruvate, 31 mM NaCl, and 2 mM GlutaMax; pH 7.4), and the cells were incubated at 37 °C in a non-CO2 incubator for 1 h. All medium and injection reagents were adjusted to pH 7.4 on the day of assay. Four baseline measurements of OCR were obtained before the sequential injection of mitochondrial inhibitors. Three readings were obtained after each addition of mitochondrial inhibitor before the injection of the subsequent inhibitors. The mitochondrial inhibitors of oligomycin (1 μM), FCCP (1 μM), and rotenone (1 μM) were used. OCR was automatically calculated and recorded using the Seahorse XF-24 software. After the assays, the plates were saved, and protein readings were measured for each well to confirm equal cell numbers per well. In comparison with the basal rates, the percentage of change was calculated as the value of change divided by the average value of baseline readings.

### 2.8. Qualitative RT-PCR

N2a cells were incubated with 5, 10, and 20 μM spermidine. After 1 h, spermidine was washed off, and 100 mM of D-Gal was added. The cells were incubated for 48 h and then were harvested. The total RNA was extracted using RNAiso Plus and reversely transcribed into cDNA using the PrimeScript RT Master Mix kit. The relative expression levels of the target and reference genes were detected using SYBR Premix Ex Taq II kit through real-time fluorescent quantitative PCR (Thermo, PikoReal 96, USA). The primer sequence is shown in Table 1.

### 2.9. Western blot

N2a cells were incubated with 5, 10, and 20 μM spermidine. After 1 h, spermidine was washed off, and 100 mM or 200 mM of D-Gal was added. The cells were incubated for 24 h or 48 h and then were harvested. The total protein was extracted using the total protein extraction kit. The protein content was measured using the Bradfold method. The loading buffer was added in the extracted samples, and the samples were boiled and denatured. The loading amount of total protein was maintained to 50 μg. The sample was separated using 10%–12% SDS-PAGE, transferred on the PVDF membrane, and blocked with 5% nonfat milk. The cleaved caspase-3 antibody (1:1000), p53 antibody (1:500), AMPK and phosphorylation AMPK antibody (1:1000), and GAPDH antibody (1:1000) were added, and the sample was incubated overnight at 4 °C. The membrane was washed with 0.01 M TBST. The corresponding secondary antibody (1:5000) was added and incubated at room temperature for 2 h. Enhanced chemiluminescence was used for development, and the relative expression was calculated using the bioanalytical imaging system (Azure Biosystem, INC., USA). The target molecular expression was quantified based on the loading control with the GAPDH expression.

### 2.10. Statistical analysis

All data are expressed as the mean ± SD of three independent measurements. Statistical analysis was performed using SPSS Statistics software 17.0. Differences between the two groups were analyzed using Student's *t*-test, whereas those among three or more groups were analyzed using one-way analysis of variance with least significant difference test. Statistical significance was considered at $p < 0.05$.

## 3. Results

### 3.1. Antiaging effect of spermidine on N2a cells following D-Gal treatment

The N2a cells viability was measured following treatment with a different dose of D-Gal for 24 h or 48 h. The cell viability decreased approximately 25% after 100 mM D-Gal treatment for 48 h compared with the control (Fig. 1A). The protective effects of spermidine on N2a cell damage induced by D-gal were tested using the MTT assay. Results showed that the pretreatment with spermidine at 10, 20, and 30 μM for 1 h improved the cell survival following 100 mM D-Gal treatment (Fig. 1B). The effects of spermidine on D-Gal induced cell aging were detected using β-galactosidase staining. After the N2a cells were treated with 100 mM of D-Gal for 48 h, the number of β-galactosidase staining-positive cells increased significantly compared with the control group ($p < 0.01$). The spermidine pretreatment reduced the number of β-galactosidase staining-positive cells compared with the single D-Gal treatment group ($p < 0.01$). This result suggested that spermidine ameliorated the D-Gal induced cell aging (Fig. 1C and D). To exclude the effect of D-Gal on cell osmosis, N2a cells were incubated with 100 mM D-glucose and 100 mM D-mannitol for 48 h, respectively. The cell aging was evaluated using the β-galactosidase staining. And result exhibited ration of positive cells in D-glucose and D-mannitol treated groups was same as in the control group (Fig. 1C, and D). The cell viability assay showed D-Gal-treatment decreased cell viability compared with the D-glucose or D-mannitol-treatment (Fig. 1E).

### 3.2. Effect of spermidine on N2a cell cycle following D-Gal treatment

The effects of spermidine on the N2a cell cycle following treatment with 100 mM D-Gal for 48 h were analyzed using flow cytometry. Results (Fig. 2A and B) showed that the N2a cells treated with 100 mM D-Gal for 48 h significantly decreased the proportion of cells in the S phase and significantly increased the proportion of cells in the G1 phase compared with the control group ($p < 0.01$). The 10, 20, and 30 μM spermidine pretreatment increased the proportion of cells in the S phase and decreased the proportion of cells in the G1 phase in a dose-dependent manner. This result suggested that spermidine improved the cell cycle arrest induced by D-Gal.

### 3.3. Protective effect of spermidine on mitochondrial damage of N2a cells induced by D-Gal

The effects of spermidine on the mitochondrial genomic stability were evaluated by detecting the mitochondrial mRNA level following the treatment with the 100 mM D-Gal for 48 h. Results (Fig. 3A) showed

**Table 1**
List of primer sequences.

| Gene name | Forward (5′-3′) | Reverse (5′-3′) |
|---|---|---|
| ATPase 6 | TCCTTCAATCCTATTCCCATCCT | ATGTTCGTCCTTTTGGTGTGTG |
| cyt b | TGGAACAACCCTAGTCGAATGAA | GTAAGATGAAGTGGAAAGCGAAGAA |
| cyt 1 | CAGACCGCAACCTAAACACAAC | GGTGCCCAAAGAATCAGAACA |
| cyt 2 | ACAAGCACAATAGATGCACAAGAAG | GCGTAGAGAGGGGAGAGCAA |
| cyt 3 | CAGGATTCTTCTGAGCGTTCTATC | AGTAGGGCTTGATTTATGTGGTTTC |
| Protein 1 | CCATTTGCAGACGCCATAAA | GGTGTGGTATTGGTAGGGGAAC |
| Protein 2 | CTATTTTCATAGGGGCATGAGGAG | AGTGAGGGATGGGTTGTAAGGA |
| Protein 3 | TGCGGATTCGACCCTACAA | TGCTCATGGTAGTGGAAGTAGAAGA |
| Protein 4 | CGATGAGGGAACCAAACTGAA | GGCAATTAGCAGTGGAATAGAACC |
| Protein 5 | TTTCCTACTGGTCCGATTCCA | TTTTGATGTCGTTTTGGGTGAG |
| Protein 6 | GCTACCCCAATCCCTCCTTC | GGTTGTGTTTGGATATACGACTGCT |
| Protein 41 | CCAATCCCCATCACCTTAGTTTT | GCATTGTAGTAGGTTGAGATTTTGG |
| Protein A61 | GCACCTTCACCAAAATCACTAACA | GGGGTAATGAATGAGGCAAATAGA |
| GAPDH | GCGAGACCCCACTAACATCAA | GTGGTTCACACCCATCACAAA |
| Grp78 | GAACACTGTGGTACCCACCAAGAA | TCCAGTCAGATCAAATGTACCCAGA |
| CHOP | AGGAGAACGAGCGGAAAGTG | GGAGAGACAGACAGGAGGTGATG |
| XBP1 | TCCCATGGACTCTGACACTGTTG | TGGGTAGACCTCTGGGAGTTCCT |
| ATF4 | GAAGAGGTCCGTAAGGCAAGG | CAGCAAACACAGCAACACAAGA |
| ATF6 | TGGAGGTCAACAAATAACACACTGG | ATTCAGTCTGCTGGTTCAGTCTGG |

that the 100 mM D-Gal treatment for 48 h significantly decreased the levels of mitochondrial mRNA in the N2a cells compared with the control group ($p < 0.01$). The 20 μM spermidine pretreatment for 1 h significantly increased the expressions levels of cy1, Cy3, Atp6, p41, P5 and P6 compared with the single D-Gal treatment groups ($p < 0.01$, or $p < 0.05$). This outcome suggested that D-Gal treatment caused mitochondrial genome damage and the spermidine treatment exerted a protective effect on the mitochondrial genome stability. The MMP was detected using Rh123 staining. The 100 mM D-Gal treated for 48 h significantly decreased the MMP of the N2a cells compared with the control group ($p < 0.05$). The spermidine pretreatment for 1 h improved the MMP in a dose-dependent manner (Fig. 3B). To further demonstrate the mitochondrial damage effect on the cell survival, the expression of cleaved caspase-3 was detected. The 100 mM D-Gal treatment for 48 h significantly increased the cleaved caspase-3 expression level in the N2a cells (Fig. 3C and E). The 5, 10, and 20 μM spermidine pretreatment for 1 h exerted an inhibitory effect on the 100 mM D-Gal-induced cleaved caspase-3 expression. The 100 mM of D-Gal treatment for 48 h significantly increased the p53 level; pretreatment with 5, 10, and 20 μM spermidine for 1 h provided an inhibitory effect on 100 mM D-Gal-induced p53 expression (Fig. 3D and F).

### 3.4. Effect of spermidine on mitochondrial function of N2a cells following D-Gal treatment

The effects of spermidine on mitochondrial respiration were evaluated by detecting the OCR following treatment with the 100 mM D-Gal for 48 h. In comparison with the control group, the OCR was significantly decreased following D-Gal treatment under the basic metabolic conditions and could be improved by spermidine pretreatment (Fig. 4A). The further administration of the ATP synthase inhibitor oligmycin (1 μM) decreased the OCR, which was significantly lower than the corresponding basic metabolic levels in all groups. However, The OCR of the single D-Gal treatment group decreased significantly ($p < 0.01$). Spermidine improved the OCR ($p < 0.05$). After treatment with the mitochondrial uncoupler FCCP (1 μM), the maximum respiratory rate was higher than the corresponding basic metabolism level. This outcome indicated that the decreased OCR level was accompanied with mitochondrial proton leak. Rotenone, the mitochondrial complex I inhibitor, could decrease the OCR to a level lower than the corresponding basal metabolic level. This finding indicated that the proportion of OCR through the nonmitochondrial pathway was extremely small. These results indicated that D-Gal significantly inhibited the mitochondrial respiratory function, and spermidine exhibited the positive effect. The ATP levels were detected using the enzyme substrate method. In comparison with the control group, the D-Gal treatment significantly decreased ATP level, whereas, the 10 and 20 μM spermidine pretreatment significantly improved the ATP level (Fig. 4B, $p < 0.05$). Given that ATP generation is regulated by AMPK phosphorylation, the levels of AMPK phosphorylation were measured using Western blot. In comparison with the control group, D-Gal treatment significantly decreased the AMPK phosphorylation level. The 5, 20, and 30 μM spermidine pretreatment increased the AMPK phosphorylation level (Fig. 4C and D).

### 3.5. Effect of spermidine on autophagy of N2a cells following D-Gal treatment

The effects of spermidine on the autophagy of the N2a cells were evaluated by detecting the LC3-2 expression following the D-Gal treatment for 8 h. After the serum was removed and cultured for 8 h, the LC3-2 expression level in the N2a cells increased significantly (Fig. 5A and B). After the D-Gal treatment for 8 h in serum-free conditions, the LC3-2 expression level decreased (Fig. 5A and B). The 5 and 20 μM spermidine treatments for 1 h improved the inhibitory effect of the 200 mM D-Gal-induced LC3-2 expression, but the improvement caused by 50 μM spermidine was not significant (Fig. 5A and B). These results suggested that the D-Gal induced neuronal aging was associated with the autophagy inhibition. Spermidine might play antiaging roles by improving the autophagy.

### 3.6. Spermidine pretreatment could not affect the endoplasmic reticulum stress of N2a cells under stress

Mitochondrial stress and endoplasmic reticulum stresses are often overlapping and associated. To further investigate whether the role of spermidine is associated with the endoplasmic reticulum stress, several molecules were measured using qRT-PCR. The levels of ATF6 and Grp78 mRNA between the D-Gal treatment group and the control group were not significantly different. The spermidine pretreatment exerted no significant influence on the expression levels of ATF6 and Grp78 (Fig. 6B and C). The levels of ATF-4, XBP-1, and CHOP between the two groups also were not significantly (Fig. 6A, D, and E). These results suggested that D-Gal induced N2a cell aging might not involve endoplasmic reticulum stress and spermidine might not depend on the unfolded protein response (UPR) signaling pathway.

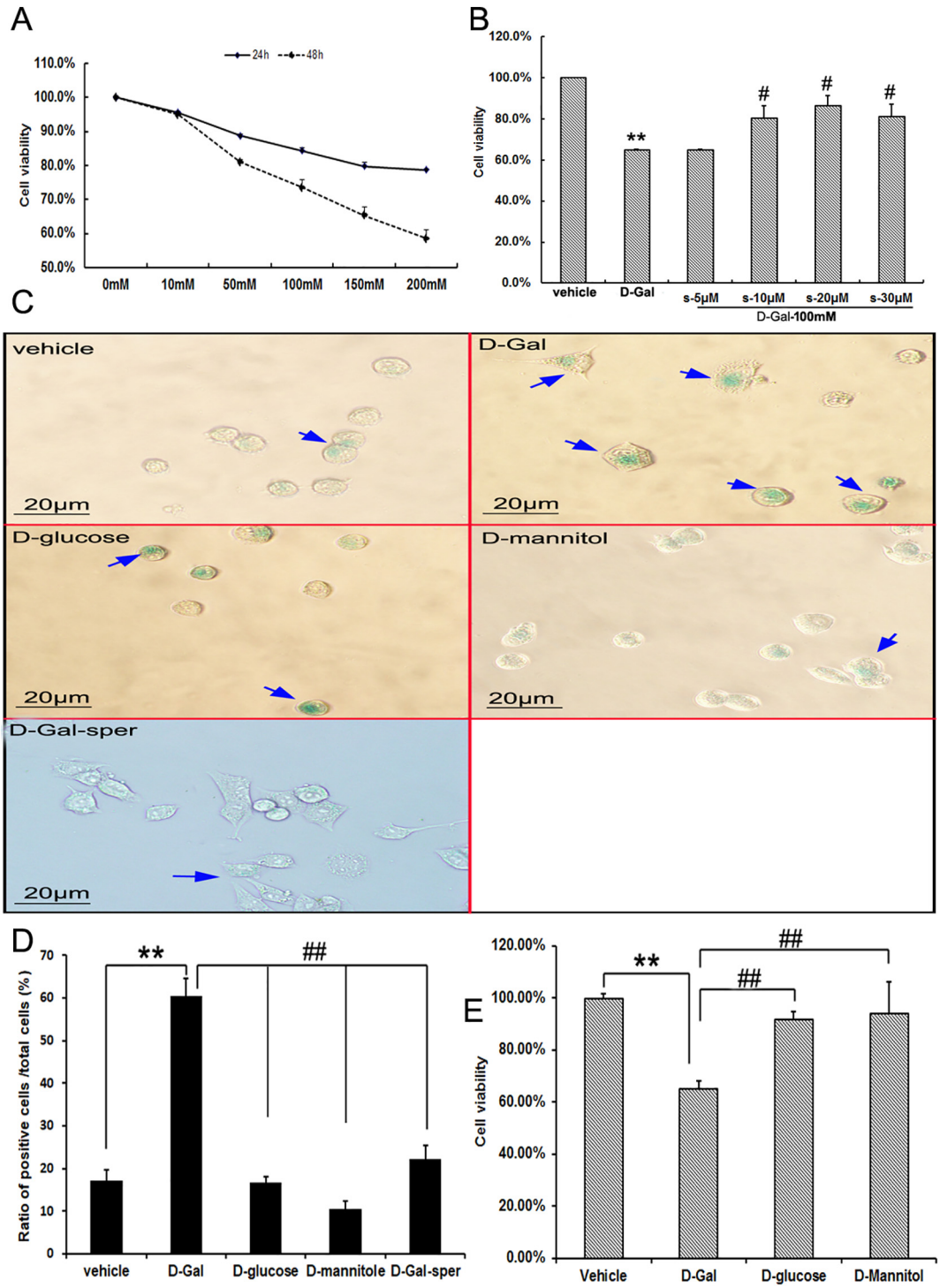


**Fig. 1.** Antiaging effects of spermidine on N2a cells following D-Gal treatment. A, cell viability was evaluated using the MTT assay following treatment with 0, 10, 50, 100, 150, 200 mM D-Gal for 24 h or 48 h. B, cell viability was determined following treatment with 5, 10, 20, 30 μM spermidine for 1 h and then incubation with D-Gal for 48 h. C, representative images of β-galactosidase staining. Vehicle group, N2a cells were cultured for 48 h with equal volume DMEM medium; D-Gal group, N2a cells were cultured for 48 h with 100 mM D-Gal; D-glucose group, N2a cells were cultured for 48 h with 100 mM D-glucose; D-mannitol group, N2a cells were cultured for 48 h with 100 mM D-mannitol; D-Gal + sper group, after incubation with 20 μM spermidine for 1 h, N2a cells were cultured for 48 h with 100 mM D-Gal; blue arrows indicate the positive cells. D, positive cell numbers of β-galactosidase staining, nine view areas per well were analyzed. E, cell viability was evaluated using the MTT method following treatment with 100 mM D-Gal and 100 mM D-glucose and 100 mM D-mannitol, respectively for 48 h. $^{**}p < 0.01$ indicates the significantly difference compared with the control group; $^{\#}p < 0.05$, $^{\#\#}p < 0.01$ indicates the significantly difference compared with the D-Gal group; $n = 3$. (For interpretation of the references to color in this figure legend, the reader is referred to the web version of this article.)

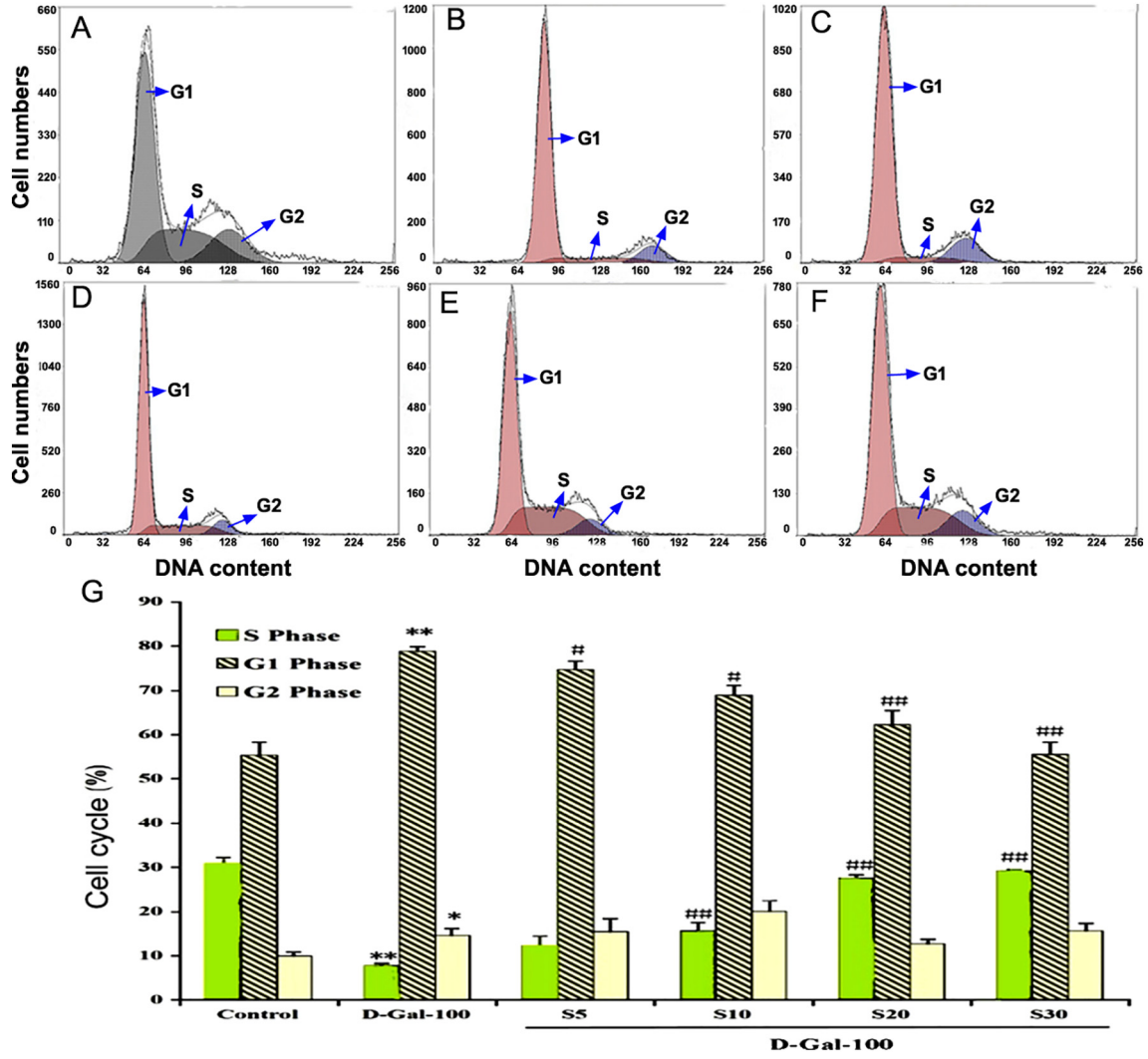


**Fig. 2.** Effect of spermidine on N2a cell cycle following D-Gal treatment. A-F, cell cycle were measured by flow cytometry. G1, cell numbers in G1 phase were computed according to the DNA content; S, cell numbers in S phase were computed according to the DNA content; G2, cell numbers in G2 phase were computed according to the DNA content. A, control group, N2a cells were cultured for 48 h without D-Gal; B, D-Gal-100 group, N2a cells were cultured for 48 h with 100 mM D-Gal; C, S5 group, after incubation with 5 μM spermidine for 1 h, N2a cells were cultured for 48 h with 100 mM D-Gal. D, S10 group, after incubation with 10 μM spermidine for 1 h, N2a cells were cultured for 48 h with 100 mM D-Gal. E, S20 group, after incubation with 20 μM spermidine for 1 h, N2a cells were cultured for 48 h with 100 mM D-Gal. F, S30 group, after incubation with 30 μM spermidine for 1 h, N2a cells were cultured for 48 h with 100 mM D-Gal. G, ratios of cell number in the S, G1, and G2 phase under the different conditions; $^{*}p < 0.05$, $^{**}p < 0.01$ indicates the significantly difference compared with the control group; $^{\#}p < 0.05$, $^{\#\#} < 0.01$ indicates the significantly difference compared with the group which was treated with single 100 mM D-Gal; $n = 3$.

## 4. Discussion

In this experiment, the N2a cells were treated with D-Gal to establish a neuronal aging model. The D-Gal-induced N2a cells were then pretreated with spermidine. Spermidine delayed the neuronal aging induced by D-Gal by improving the mitochondrial genome stability and MMP, promoting the utilization of oxygen and inhibiting cell apoptosis. D-Gal can cause abnormal increases in intracellular galactose, glucose metabolism disorder, abnormal energy production and accelerated cell aging (Lei et al., 2008). D-gal is a reduced monosaccharide. At normal concentrations, it is metabolized into glucose, but at higher doses, it is converted into aldose and hydroperoxide resulting in the formation of reactive oxygen species (Wu et al., 2008).

Neuronal aging have several causes, such as decreased genomic stability, reduced DNA repair function, telomere shortening caused by telomerase deletion, sepigenetic alterations, and multiple protein misfolding. Mitochondrial morphology and function abnormalities are associated with aging. However, whether mitochondrial abnormalities cause aging or aging exacerbated mitochondrial abnormalities is still unclear. Mitochondria have their own DNA and the characteristics of semiconservative replication. mtDNA is more vulnerable to damage due to a self-repair deficit. A long-standing hypothesis postulates that mutations in the mitochondrial genome limit mammalian life span (Linnane et al., 1989). Harboring a proofreading-deficient copy of the catalytic subunit of polymerase gamma (PolgA) provides a unique opportunity to test the validity of this hypothesis and to dissect the role of PolgA in mitochondrial mutagenesis. Homozygous carriers of the proofreading -deficient PolgA allele ($PolgA^{mut/mut}$) show several features of accelerated aging, whereas heterozygous mice ($PolgA^{+/mut}$) do not (Ross et al., 2013). In one study, a random mutation capture technology showed that the mtDNA in the brain and heart tissues exhibited a large age-dependent deletion (Vermulst et al., 2008a). This deletion had already appeared in the early stage of life and showed a cumulative effect with increasing age. Simultaneously, the expression level of mtDNA encoding cytochrome oxidase was decreased (Vermulst et al., 2008b). In another research with the same animal model, the deletion frequency of 8 kb mtDNA in the brain greatly increased in mice at 15 month postnatal period as detected using single molecule PCR

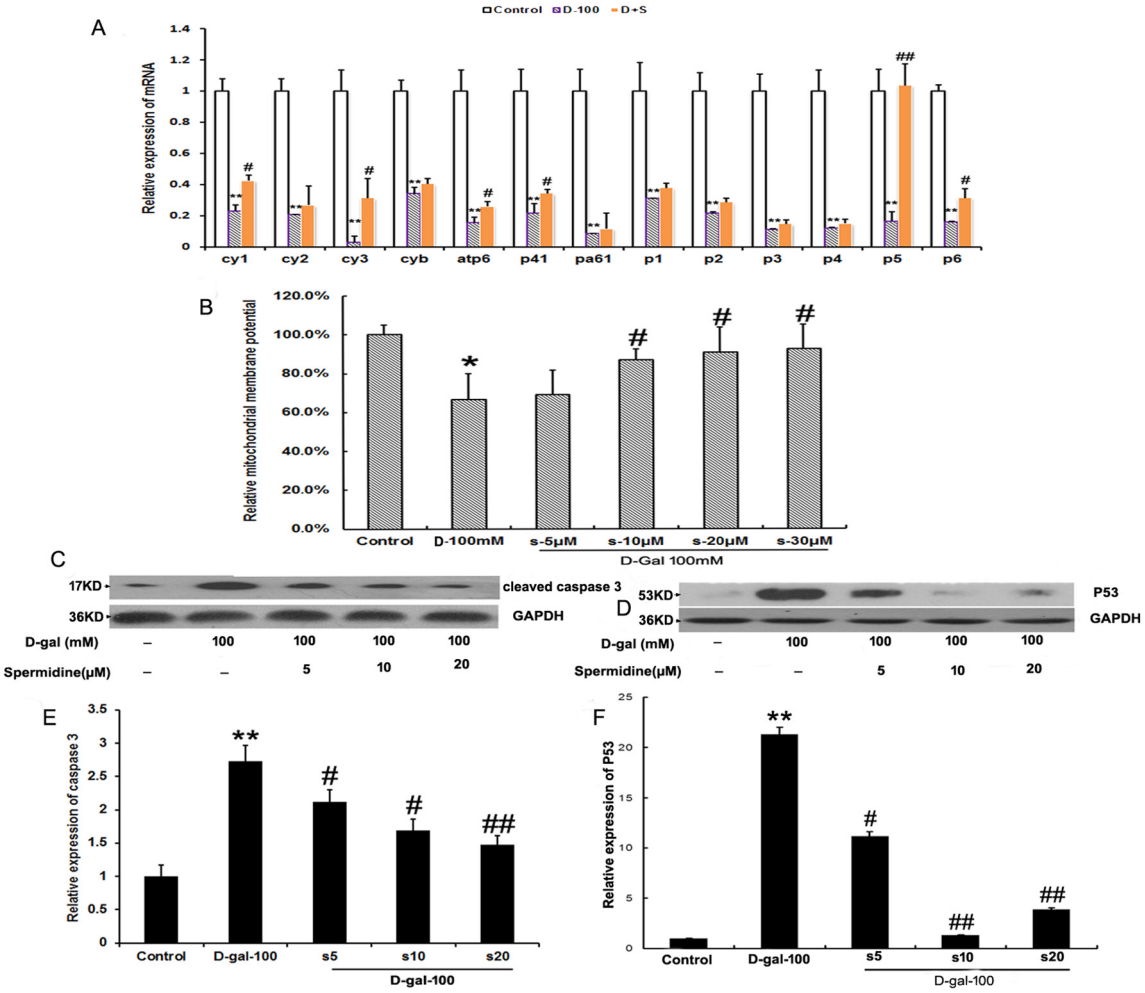


**Fig. 3.** Protective effect of spermidine on mitochondrial damage of N2a cells induced by D-Gal. A, N2a cells incubated with 20 μM spermidine. After 1 h, spermidine was washed off, and 100 mM D-Gal was added and incubated for 48 h. Expression levels of mRNA encoded by mtDNA were analyzed with qRT-PCR. Control group, N2a cells were cultured for 48 h without D-Gal; D-100 group, N2a cells were cultured for 48 h with 100 mM D-Gal; D + S group, after incubation with 20 μM spermidine for 1 h, N2a cells were cultured for 48 h with 100 mM D-Gal. B. MMP was analyzed. N2a cells incubated with 5, 10, 20, and 30 μM spermidine. After 1 h, spermidine was washed off, and 100 mM D-Gal was added and incubated for 48 h. C and E, expression levels of cleaved caspase-3. N2a cells incubated with 5, 10, and 20 μM spermidine. After 1 h, spermidine was washed off, and 100 mM D-Gal was added and incubated for 48 h. C, representative images of Western blot; E, relative expression of cleaved caspase-3 was analyzed. D and F, expression levels of p53. N2a cells incubated with 5, 10 and 20 μM spermidine. After 1 h, spermidine was washed off, and 100 mM D-Gal was added and incubated for 48 h. D, representative images of Western blot; F, relative expression of p53 was analyzed. $^{*}p < 0.05$, $^{**}p < 0.01$ indicate the significantly difference compared with the control group; $^{\#}p < 0.05$, $^{\#\#} < 0.01$ indicate the significantly difference compared with the group which was treated with single 100 mM D-Gal; n = 3.

(Kraytsberg et al., 2009). In a study on the brain of aged rats, the expression levels of 7S DNA in D-loop decreased; such decrease is associated with the known age-related decline in mitochondrial oxidative phosphorylation (McInerny et al., 2009). A study on rhesus also found that the proportion of 5.7 kb deletion in the cerebral cortex increased in aged rhesus (21–33 years old) compared with the young adults (3–5 years old) (Mao et al., 2012). Age-dependent neurodegenerative diseases also manifest the characteristics of mtDNA damage. The mtDNA deletion in the substantia nigra and striatum of patients with PD is approximately 40%, the activity of respiratory chain complex I is decreased, and the gene of the coding complex I subunit is reduced (Papa et al., 2009). Mitochondrial oxidative phosphorylation deficiency is also observed in patients with AD (Mancuso et al., 2010). The activity of respiratory chain complex IV is decreased and mtDNA point mutation and fragment deletion are increased in patients with AD (Yang et al., 2012). Mitochondrial respiratory chain complex IV defect is also found in some patients with Huntington disease (Mehrotra et al., 2015). Similarly, mtDNA damage is a hallmark in animal models of Huntingtons' disease (Acevedo-Torres et al., 2009). By using a D-Gal-induced animal aging model, Kong's study found that mtDNA mutation and deletion in the animal's auditory cortex (Chen et al., 2010). The structural properties and replication characteristics of mtDNA determine the susceptibility of mtDNA to injury factors, especially in the organ with active oxidative phosphorylation. Moreover, the pathology of mtDNA injury depends on the frequency and quantity of mtDNA mutation. Our results showed that expression levels of 13 mRNAs encoded by the mtDNA decreased with decreasing MMP following the D-Gal treatment. The spermidine treatment alleviated the decrease of mitochondrial mRNA expression and also improved the MMP, which initiated the mitochondrial dependent apoptosis. The D-Gal treatment increased the cleaved caspase-3 expression level, whereas spermidine pretreatment partially inhibited it in a dose-dependent manner. Similarly, the D-Gal treatment increased the p53 expression level, whereas spermidine decreased it in a dose-dependent manner. P53 may activate the downstream apoptotic signaling proteins, such as Bcl-2; initiate the apoptosis; block the cell cycle; and start the repair mechanism (Floriddia et al., 2012). In the present study, the D-Gal induced N2a cell cycle arrest and spermidine exerted a certain improvement effect. These

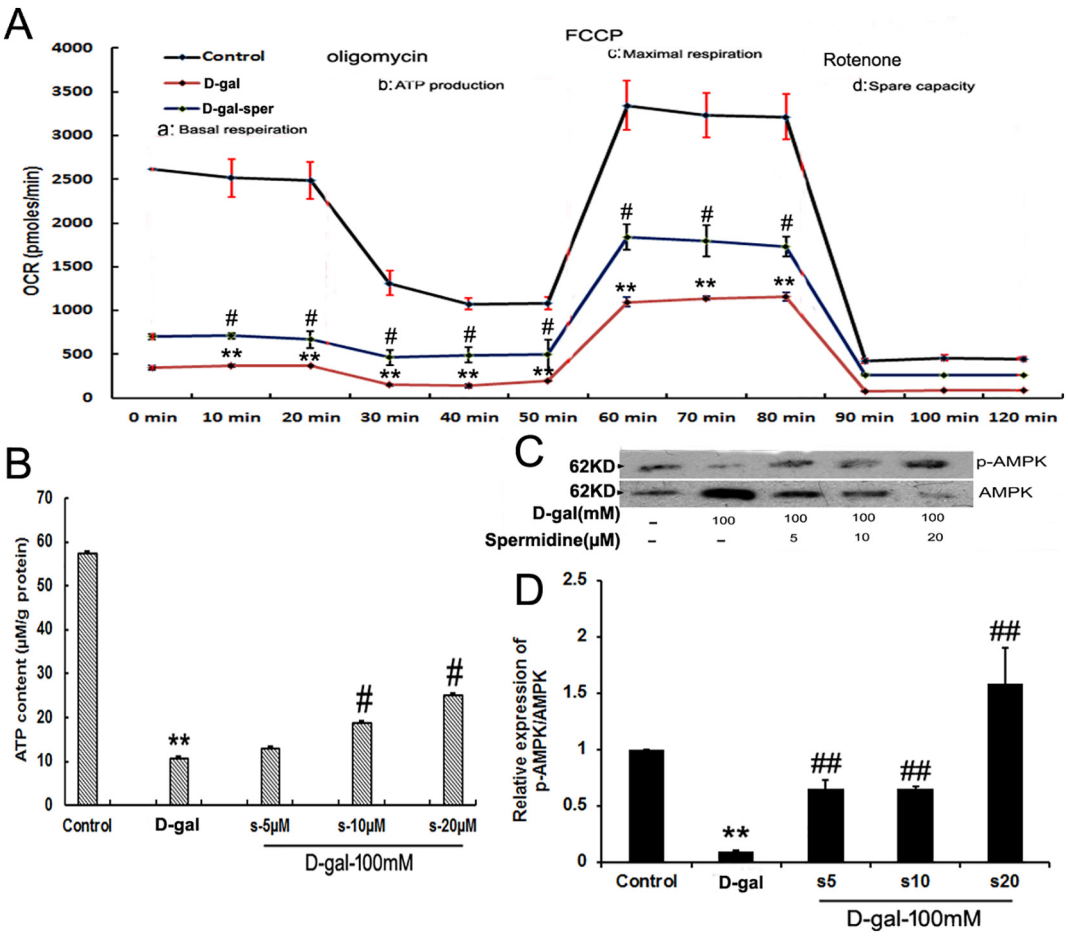


**Fig. 4.** Effect of spermidine on mitochondrial function of N2a cells following D-Gal treatment. A, OCR was analyzed using Seahorse XF-24 Metabolic Flux Analysis system. N2a cells incubated with 20 μM spermidine. After 1 h, spermidine was washed off, and 100 mM D-Gal was added and incubated for 48 h. a. basic OCR; b. incubation with 1 μM oligmycin; c. incubation with 1 μM FCCP; d. incubation with 1 μM rotenone. Control group, N2a cells were cultured for 48 h without D-Gal; D-100 group, N2a cells were cultured for 48 h with 100 mM D-Gal; D + S group, after incubation with 20 μM spermidine for 1 h, N2a cells were cultured for 48 h with 100 mM D-Gal. B, ATP contents were measured. N2a cells incubated with 5, 10, and 20 μM spermidine. After 1 h, spermidine was washed off, and 100 mM D-Gal was added and incubated for 48 h. C and D, ratio of phosphorylation AMPK to total AMPK. N2a cells incubated with 5, 10, and 20 μM spermidine. After 1 h, spermidine was washed off, and 100 mM D-Gal was added and incubated for 48 h. C, representative images of Western blot; D, relative expression of phosphorylation AMPK was analyzed. $^{**}p < 0.01$ indicates the significantly difference compared with the control group; $^{\#}p < 0.05$, $^{\#\#} < 0.01$ indicate the significantly difference compared with the group which was treated with single 100 mM D-Gal; n = 3.

results suggested that spermidine possibly resisted the cell aging by protecting the mitochondrial damage, stabilizing the mitochondrial genome and membrane potential, and reducing the apoptosis and cell cycle arrest. Nevertheless, in the work of Li et al., N2a cells incubated with D-gal exhibited increased cell death through necroptosis but not apoptosis (Li et al., 2011). This discrepancy may be attributed to the different protocols including D-gal dose, treatment time, and test methods. A high dose of D-gal was used in Li et al.'s work and possibly directly induced cell necroptosis by damaging the cell membrane.

The generation and utilization of energy are closely related to the mitochondrial function, and a deficit of energy utilization is also an important reason for aging (Barzilai et al., 2012). Among drugs that exert the antiaging effects, resveratrol and metformin can improve mitochondrial oxidative phosphorylation, improve the AMPK sensitivity, and reduce the free radicals accumulation (Chen et al., 2017; Palomera-Avalos et al., 2017). In this study, the level of OCR was determined. D-Gal significantly inhibited the cell oxygen utilization and reduced the ATP production, but both were improved by spermidine. D-Gal also inhibited the AMPK phosphorylation in the N2a cells, which was also improved by spermidine. AMPK activation can induce the autophagy (Herzig and Shaw, 2017). In the present study, spermidine improved the inhibitory effect of D-Gal on autophagy. These results suggested that the antiaging effect of spermidine was intimately related to cell metabolism, which might enhance the utilization of oxygen by sensitizing the cellular energy. The effect of spermidine depends on its deacetylation of histone-3 which influence the expression of nuclear genes (Madeo et al., 2010). Age-dependent decline in brain polyamine levels results in the impairment of memory performance in Drosophila, which can be counteracted by external administration of spermidine. Hence, spermidine has a potential role in improving age-related neurodegeneration (Sigrist et al., 2014).

## 5. Conclusion

Although the present investigation was limited to the cellular level, this study showed that spermidine ameliorated the neural aging associated with changes in mitochondrial structure and function following stress. Spermidine pretreatment delayed the D-Gal-induced in the N2a cells through the maintenance of mitochondrial genome stability and MMP, inhibition of apoptosis signal activation, improvement of mitochondrial function and improvement of oxygen utilization and autophagy. The protective effect of spermidine was not dependent on the UPR signaling pathway.

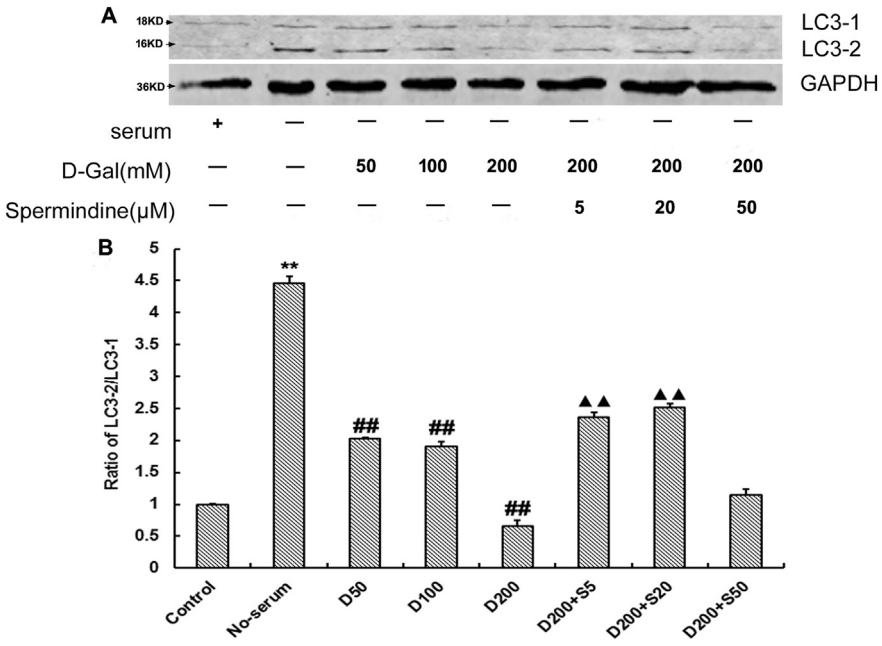


**Fig. 5.** Effect of spermidine on autophagy of N2a cells following D-Gal treatment. N2a cells were cultured with or without serum, and incubated with 5, 10, and 20 μM spermidine. After 1 h, spermidine was washed off, and 50, 100, and 200 mM D-Gal was added and incubated for 8 h. A, representative images of Western blot; B, relative expression of LC3-2 was analyzed. $^{**}p < 0.01$ indicates the significantly difference compared with the control group; $^{\#\#} < 0.01$ indicates the significantly difference compared with the group without serum; ▲▲$p < 0.01$ indicates the significantly difference compared with the group without serum; n = 3.

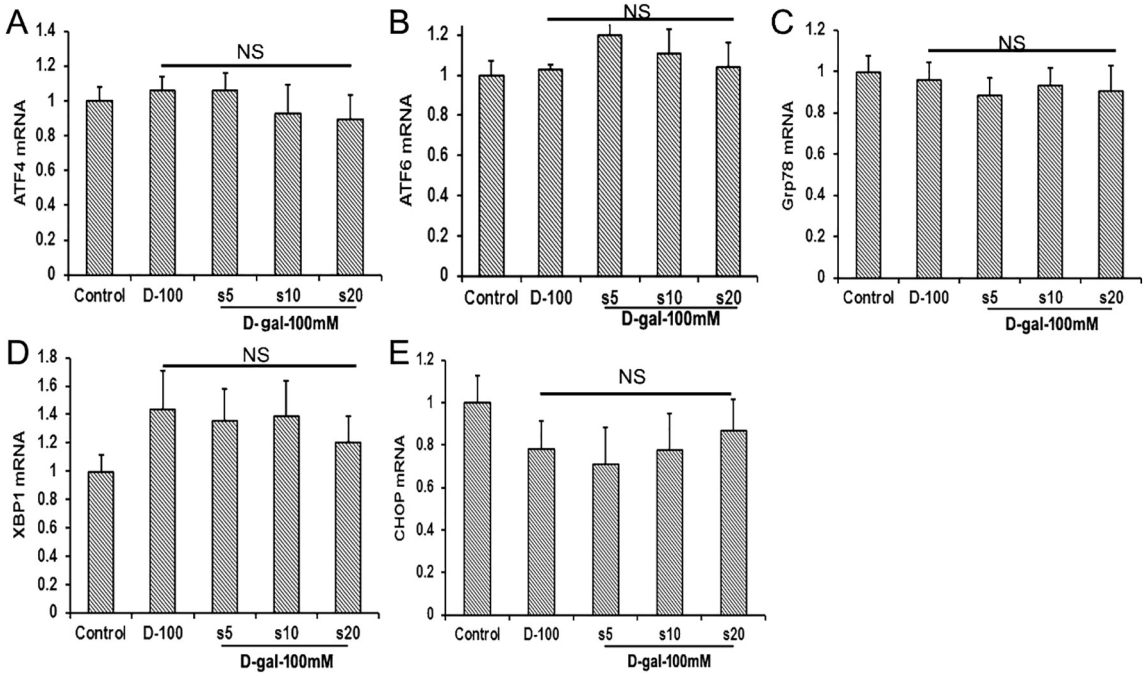


**Fig. 6.** Spermidine pretreatment could not affect the endoplasmic reticulum stress of N2a cells under stress. N2a cells incubated with 5, 10, and 20 μM spermidine. After 1 h, spermidine was washed off, and 100 mM D-Gal was added and incubated for 48 h. A, relative expression level of ATF4 mRNA. B, relative expression level of ATF6 mRNA. C, relative expression level of Grp78 mRNA. D. relative expression level of XBP1 mRNA. E, relative expression level of CHOP mRNA. NS, $p > 0.05$ indicates no significantly difference between groups; n = 3.

## Conflict of interests

The authors declare that there is no conflict of interests regarding the publication of this paper.

## Acknowledgments

This work is partly supported by National Natural Science Foundation of China (No. 81370448 and 81570725) to Jing Yu Hong.

## References

Acevedo-Torres, K., Berrios, L., Rosario, N., Dufault, V., Skatchkov, S., Eaton, M.J., Torres-Ramos, C.A., Ayala-Torres, S., 2009. Mitochondrial DNA damage is a hallmark of chemically induced and the R6/2 transgenic model of Huntington's disease. DNA Repair 8, 126–136.

Barzilai, N., Huffman, D.M., Muzumdar, R.H., Bartke, A., 2012. The critical role of metabolic pathways in aging. Diabetes 61, 1315–1322.

Basha, P.M., Poojary, A., 2014. Mitochondrial dysfunction in aging rat brain regions upon chlorpyrifos toxicity and cold stress: an interactive study. Cell. Mol. Neurobiol. 34, 737–756.

Bell, M.R., Belarde, J.A., Johnson, H.F., Aizenman, C.D., 2011. A neuroprotective role for polyamines in a Xenopus tadpole model of epilepsy. Nat. Neurosci. 14, 505–512.

Biedermann, B., Skatchkov, S.N., Brunk, I., Bringmann, A., Pannicke, T., Bernstein, H.G.,

Faude, F., Germer, A., Veh, R., Reichenbach, A., 1998. Spermine/spermidine is expressed by retinal glial (Muller) cells and controls distinct $K^+$ channels of their membrane. Glia 23, 209–220.
Chen, B., Zhong, Y., Peng, W., Sun, Y., Kong, W.J., 2010. Age-related changes in the central auditory system: comparison of D-galactose-induced aging rats and naturally aging rats. Brain Res. 1344, 43–53.
Chen, J., Ou, Y., Li, Y., Hu, S., Shao, L.W., Liu, Y., 2017. Metformin Extends *C. elegans* Lifespan Through Lysosomal Pathway. pp. 6.
Childs, A.C., Mehta, D.J., Gerner, E.W., 2003. Polyamine-dependent gene expression. Cell. Mol. Life Sci. 60, 1394–1406.
Delwing-de Lima, D., Hennrich, S.B., Delwing-Dal Magro, D., Aurelio, J.G., Serpa, A.P., Augusto, T.W., Pereira, N.R., 2017. The effect of D-galactose induced oxidative stress on in vitro redox homeostasis in rat plasma and erythrocytes. Biomed. Pharmacother. 86, 686–693.
Eisenberg, T., Knauer, H., Schauer, A., Buttner, S., Ruckenstuhl, C., Carmona-Gutierrez, D., Ring, J., Schroeder, S., Magnes, C., Antonacci, L., et al., 2009. Induction of autophagy by spermidine promotes longevity. Nat. Cell Biol. 11, 1305–1314.
Floriddia, E.M., Rathore, K.I., Tedeschi, A., Quadrato, G., Wuttke, A., Lueckmann, J.M., Kigerl, K.A., Popovich, P.G., Di Giovanni, S., 2012. p53 Regulates the neuronal intrinsic and extrinsic responses affecting the recovery of motor function following spinal cord injury. J. Neurosci. 32, 13956–13970.
Gems, D., Partridge, L., 2013. Genetics of longevity in model organisms: debates and paradigm shifts. Annu. Rev. Physiol. 75, 621–644.
Gosule, L.C., Schellman, J.A., 1976. Compact form of DNA induced by spermidine. Nature 259, 333–335.
Herzig, S., Shaw, R.J., 2017. AMPK: guardian of metabolism and mitochondrial homeostasis. Nat. Rev. Mol. Cell Biol. 19, 121–135.
Kenyon, C.J., 2010. The genetics of ageing. Nature 464, 504–512.
Khomutov, A.R., Keinanen, T.A., Grigorenko, N.A., Hyvonen, M.T., Uimari, A., Pietila, M., Cerrada-Gimenez, M., Simonian, A.R., Khomutov, M.A., Verspalainen, J., et al., 2009. Methylated analogues of spermine and spermidine as tools to investigate cellular functions of polyamines and the enzymes of their metabolism. Mol. Biol. 43, 274–285.
Krauss, M., Weiss, T., Langnaese, K., Richter, K., Kowski, A., Veh, R.W., Laube, G., 2007. Cellular and subcellular rat brain spermidine synthase expression patterns suggest region-specific roles for polyamines, including cerebellar pre-synaptic function. J. Neurochem. 103, 679–693.
Kraytsberg, Y., Simon, D.K., Turnbull, D.M., Khrapko, K., 2009. Do mtDNA deletions drive premature aging in mtDNA mutator mice? Aging Cell 8, 502–506.
de Lau, L.M., Giesbergen, P.C., de Rijk, M.C., Hofman, A., Koudstaal, P.J., Breteler, M.M., 2004. Incidence of parkinsonism and Parkinson disease in a general population: the Rotterdam Study. Neurology 63, 1240–1244.
Laube, G., Veh, R.W., 1997. Astrocytes, not neurons, show most prominent staining for spermidine/spermine-like immunoreactivity in adult rat brain. Glia 19, 171–179.
Lauri, A., Pompilio, G., Capogrossi, M.C., 2014. The mitochondrial genome in aging and senescence. Ageing Res. Rev. 18, 1–15.
Lei, M., Hua, X., Xiao, M., Ding, J., Han, Q., Hu, G., 2008. Impairments of astrocytes are involved in the D-galactose-induced brain aging. Biochem. Biophys. Res. Commun. 369, 1082–1087.
Li, N., He, Y., Wang, L., Mo, C., Zhang, J., Zhang, W., Li, J., Liao, Z., Tang, X., Xiao, H., 2011. D-Galactose induces necroptotic cell death in neuroblastoma cell lines. J. Cell. Biochem. 112, 3834–3844.
Li, J., Zhang, C.C., Yang, L., Wang, T., Zhou, Z.Y., Yuan, D., Dun, Y.Y., 2014. Protective effect of total flavonoids of epimedium on D-galactose-induced senescence in H9c2 cells. Zhong Yao Cai 37, 2255–2258.
Linnane, A.W., Marzuki, S., Ozawa, T., Tanaka, M., 1989. Mitochondrial DNA mutations as an important contributor to ageing and degenerative diseases. Lancet 1, 642–645.
Lopez-Otin, C., Blasco, M.A., Partridge, L., Serrano, M., Kroemer, G., 2013. The hallmarks of aging. Cell 153, 1194–1217.
Lopez-Otin, C., Galluzzi, L., Freije, J.M.P., Madeo, F., Kroemer, G., 2016. Metabolic control of longevity. Cell 166, 802–821.
Macedo, J.C., Vaz, S., Logarinho, E., 2017. Mitotic dysfunction associated with aging hallmarks. Adv. Exp. Med. Biol. 1002, 153–188.
Madeo, F., Eisenberg, T., Buttner, S., Ruckenstuhl, C., Kroemer, G., 2010. Spermidine: a novel autophagy inducer and longevity elixir. Autophagy 6, 160–162.
Mancuso, M., Orsucci, D., LoGerfo, A., Calsolaro, V., Siciliano, G., 2010. Clinical features and pathogenesis of Alzheimer's disease: involvement of mitochondria and mitochondrial DNA. Adv. Exp. Med. Biol. 685, 34–44.
Mao, P., Gallagher, P., Nedungadi, S., Manczak, M., Shirendeb, U.P., Kohama, S.G., Ferguson, B., Park, B.S., Reddy, P.H., 2012. Mitochondrial DNA deletions and differential mitochondrial DNA content in rhesus monkeys: implications for aging. Biochim. Biophys. Acta 1822, 111–119.
McInerny, S.C., Brown, A.L., Smith, D.W., 2009. Region-specific changes in mitochondrial D-loop in aged rat CNS. Mech. Ageing Dev. 130, 343–349.
Mehrotra, A., Kanwal, A., Banerjee, S.K., Sandhir, R., 2015. Mitochondrial modulators in experimental Huntington's disease: reversal of mitochondrial dysfunctions and cognitive deficits. Neurobiol. Aging 36, 2186–2200.
Minois, N., 2014. Molecular basis of the 'anti-aging' effect of spermidine and other natural polyamines - a mini-review. Gerontology 60, 319–326.
Minois, N., Carmona-Gutierrez, D., Bauer, M.A., Rockenfeller, P., Eisenberg, T., Brandhorst, S., Sigrist, S.J., Kroemer, G., Madeo, F., 2012. Spermidine promotes stress resistance in *Drosophila* melanogaster through autophagy-dependent and -independent pathways. Cell Death Dis. 3, e401.
Noro, T., Namekata, K., Kimura, A., Guo, X., Azuchi, Y., Harada, C., Nakano, T., Tsuneoka, H., Harada, T., 2015. Spermidine promotes retinal ganglion cell survival and optic nerve regeneration in adult mice following optic nerve injury. Cell Death Dis. 6, e1720.
Palomera-Avalos, V., Grinan-Ferre, C., Izquierdo, V., Camins, A., Sanfeliu, C., Pallas, M., 2017. Metabolic stress induces cognitive disturbances and inflammation in aged mice: protective role of resveratrol. Rejuvenation Res. 20, 202–217.
Papa, S., Petruzzella, V., Scacco, S., Sardanelli, A.M., Iuso, A., Panelli, D., Vitale, R., Trentadue, R., De Rasmo, D., Capitanio, N., et al., 2009. Pathogenetic mechanisms in hereditary dysfunctions of complex I of the respiratory chain in neurological diseases. Biochim. Biophys. Acta 1787, 502–517.
Pegg, A.E., 1988. Polyamine metabolism and its importance in neoplastic growth and a target for chemotherapy. Cancer Res. 48, 759–774.
Ross, J.M., Stewart, J.B., Hagstrom, E., Brene, S., Mourier, A., Coppotelli, G., Freyer, C., Lagouge, M., Hoffer, B.J., Olson, L., et al., 2013. Germline mitochondrial DNA mutations aggravate ageing and can impair brain development. Nature 501, 412–415.
Rubinsztein, D.C., Easton, D.F., 1999. Apolipoprotein E genetic variation and Alzheimer's disease. A meta-analysis. Dement. Geriatr. Cogn. Disord. 10, 199–209.
Sano, M., Ernesto, C., Thomas, R.G., Klauber, M.R., Schafer, K., Grundman, M., Woodbury, P., Growdon, J., Cotman, C.W., Pfeiffer, E., et al., 1997. A controlled trial of selegiline, alpha-tocopherol, or both as treatment for Alzheimer's disease. The Alzheimer's disease cooperative study. N. Engl. J. Med. 336, 1216–1222.
Sigrist, S.J., Carmona-Gutierrez, D., Gupta, V.K., Bhukel, A., Mertel, S., Eisenberg, T., Madeo, F., 2014. Spermidine-triggered autophagy ameliorates memory during aging. Autophagy 10, 178–179.
Skatchkov, S.N., Eaton, M.J., Krusek, J., Veh, R.W., Biedermann, B., Bringmann, A., Pannicke, T., Orkand, R.K., Reichenbach, A., 2000. Spatial distribution of spermine/spermidine content and K(+)-current rectification in frog retinal glial (Muller) cells. Glia 31, 84–90.
Skatchkov, S.N., Woodbury-Farina, M.A., Eaton, M., 2014. The role of glia in stress: polyamines and brain disorders. Psychiatr. Clin. North Am. 37, 653–678.
Soda, K., Dobashi, Y., Kano, Y., Tsujinaka, S., Konishi, F., 2009. Polyamine-rich food decreases age-associated pathology and mortality in aged mice. Exp. Gerontol. 44, 727–732.
Trifunovic, A., Wredenberg, A., Falkenberg, M., Spelbrink, J.N., Rovio, A.T., Bruder, C.E., Bohlooly, Y.M., Gidlof, S., Oldfors, A., Wibom, R., et al., 2004. Premature ageing in mice expressing defective mitochondrial DNA polymerase. Nature 429, 417–423.
Vermulst, M., Bielas, J.H., Loeb, L.A., 2008a. Quantification of random mutations in the mitochondrial genome. Methods 46, 263–268.
Vermulst, M., Wanagat, J., Kujoth, G.C., Bielas, J.H., Rabinovitch, P.S., Prolla, T.A., Loeb, L.A., 2008b. DNA deletions and clonal mutations drive premature aging in mitochondrial mutator mice. Nat. Genet. 40, 392–394.
Wang, X., Levic, S., Gratton, M.A., Doyle, K.J., Yamoah, E.N., Pegg, A.E., 2009. Spermine synthase deficiency leads to deafness and a profound sensitivity to alpha-difluoromethylornithine. J. Biol. Chem. 284, 930–937.
Xing, Y., Yang, L., Lin, H., 2006. Study on cell senescence induced by D-galactose in cultured rat mesenchymal stem cells. Zhongguo Xiu Fu Chong Jian Wai Ke Za Zhi 20, 475–479.
Yang, L., Ye, C.Y., Huang, X.T., Tang, X.C., Zhang, H.Y., 2012. Decreased accumulation of subcellular amyloid-beta with improved mitochondrial function mediates the neuroprotective effect of huperzine A. J. Alzheimers Dis. 31, 131–142.
Yao, J., Irwin, R.W., Zhao, L., Nilsen, J., Hamilton, R.T., Brinton, R.D., 2009. Mitochondrial bioenergetic deficit precedes Alzheimer's pathology in female mouse model of Alzheimer's disease. Proc. Natl. Acad. Sci. U. S. A. 106, 14670–14675.
Zhang, D., Yan, B., Yu, S., Zhang, C., Wang, B., Wang, Y., Wang, J., Yuan, Z., Zhang, L., Pan, J., 2015. Coenzyme Q10 inhibits the aging of mesenchymal stem cells induced by D-galactose through Akt/mTOR signaling. Oxidative Med. Cell. Longev. 2015, 867293.
Zhao, G.R., Zhang, H.M., Ye, T.X., Xiang, Z.J., Yuan, Y.J., Guo, Z.X., Zhao, L.B., 2008. Characterization of the radical scavenging and antioxidant activities of danshensu and salvianolic acid B. Food Chem. Toxicol. 46, 73–81.
Wu, D.M., Lu, J., Zheng, Y.L., Zhou, Z., Shan, Q., Ma, D.F., 2008. Purple sweet potato color repairs D-galactose-induced spatial learning and memory impairment by regulating the expression of synaptic proteins. Neurobiol. Learn. Mem. 90, 19–27.